Marine Pollution Bulletin 156 (2020) 111229

Contents lists available at ScienceDirect

Marine Pollution Bulletin

journal homepage: www.elsevier.com/locate/marpolbul

Modelling of oil thickness in the presence of an ice edge

Tor Nordam[a,b,*], Emma Litzler[a], Jørgen Skancke[a], Ivar Singsaas[a], Frode Leirvik[a], Øistein Johansen[c]

[a] SINTEF Ocean, Trondheim, Norway
[b] Department of Physics, Norwegian University of Science and Technology, Trondheim, Norway
[c] JEMC, Trondheim, Norway

ARTICLE INFO

Keywords:
Oil in ice
Oil spill modelling
Oil spill trajectory
Arctic oil spill response

ABSTRACT

Oil slick thickness is a key parameter for the behaviour of oil spilled at sea. It influences evaporation and entrainment, viable response options, and the risk to marine life at the surface. Determining this value is therefore of high relevance in oil spill modelling. In open water, oil can spread as thin films due to gravity alone, and may be further dispersed by horizontal diffusion and differential advection. In the presence of ice, however, a thin oil slick may become concentrated to higher thickness, if compressed against the ice edge.

In the present study, we develop a simple model for the thickness of oil forced against a barrier by a current. We compare our theory to flume experiments, and obtain reasonable agreement. We describe an implementation in a Lagrangian oil spill model, and present some examples. We discuss the operational applicability, and suggest further research needs.

1. Introduction

Oil spill modelling is commonly used to assist planning of contingency and response options in case of accidental oil spills during production or exploration. The aim of modelling in the planning phase is to predict probable locations where the oil will end up, and to quantify how much oil might be stranded, submerged, or remain at the surface. A key target for modelling is to predict the state of surface oil, as this impacts the further fate of the spill and what response options are viable. In an operational phase, *i.e.*, during an ongoing oil spill response operation, the goals are similar, but on a shorter timescale, and with more focus on directing response operations.

A complete marine oil spill model must account for a range of processes that affect oil at sea, including spreading, transport, mixing, evaporation, emulsification, and biodegradation. If ice is present, many of these processes are modified in some way (see, *e.g.*, Afenyo et al. (2016a)). For example, oil in a broken ice field tends to evaporate and emulsify more slowly than oil in open water, due to reduced surface area and typically low temperatures (Brandvik and Faksness, 2009). Biodegradation rates are also reduced in low temperatures (Bagi et al., 2013; Lofthus et al., 2018; Nordam et al., 2020).

The transport of oil at the surface changes from being controlled mainly by the wind at low ice coverage, to being controlled by the ice at high coverage (El-Tahan et al., 1988; Venkatesh et al., 1990; French-McCay et al., 2014; French-McCay et al., 2018; Nordam et al., 2019). In scenarios where ice is present, ice cover is also strongly correlated to many of the endpoints of an oil spill simulation used in risk assessment (Arneborg et al., 2017; Nordam et al., 2017), highlighting a need for accurate ice data, and accurate modelling of oil-ice interactions. See, *e.g.*, Afenyo et al. (2016b) for a recent review of how oil spills are affected by the presence of ice.

The topic of the current study is the modelling of oil thickness in the presence of an ice edge, based on recent experimental work (Singsaas et al., 2020). While both oil and sea ice are moved by the wind and current, they move differently, and in some cases oil that is spilled close to sea ice will be transported into the marginal ice zone (MIZ). In such cases, surface oil that is initially thin can be concentrated to higher thickness. This is somewhat similar to what happens when a boom is used to collect oil during response operations.

The increased thickness may have implications for which response options are actionable, and may affect the future fate of the oil even if no response actions are taken. Hence, it is of some interest to accurately model the thickness of oil against an ice edge.

The layout of this paper is as follows: In Section 2, we describe our development of a model for the thickness of oil in the presence of an ice edge. In Section 3, we describe experimental work that was undertaken to validate the theory. The implementation of our theory into a particle-based oil spill model is outlined in Section 4, and in Section 5, we

* Corresponding author at: SINTEF Ocean, Trondheim, Norway.
E-mail address: tor.nordam@sintef.no (T. Nordam).

https://doi.org/10.1016/j.marpolbul.2020.111229
Received 31 January 2020; Received in revised form 23 April 2020; Accepted 26 April 2020
Available online 23 May 2020

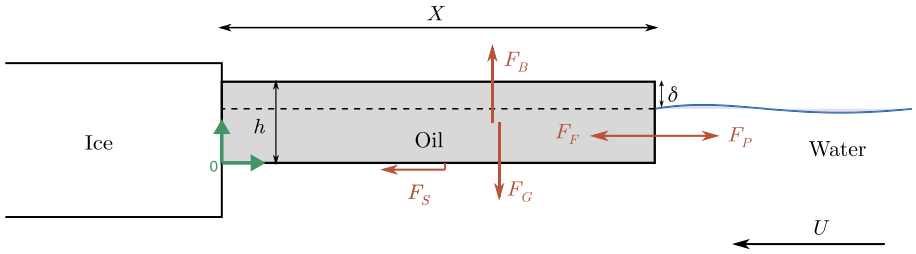

Fig. 1. Representation of an oil slick against an ice edge. U is the water current pushing the oil towards the edge. The relevant forces are shown in red: The skin friction F_S, the form drag F_F, the pressure force of the oil on the water F_P, the gravitational force on the oil F_G, and the buoyancy force on the oil F_B. (For interpretation of the references to colour in this figure legend, the reader is referred to the web version of this article.)

provide some discussion of the relevance and applicability of the new approach. Finally, in Section 6 we draw some conclusions.

2. Theory

In what follows, we will develop a model to calculate the equilibrium thickness of oil, being pushed against an ice edge (or any other floating barrier) by a constant current. We will assume that the oil can be described as a Newtonian fluid, and by formulating an equilibrium model, we also make the implicit assumption that the oil will reach its equilibrium thickness relatively fast, compared to other timescales in the problem.

We consider an oil slick of even thickness, h, against an ice edge, as shown in Fig. 1. We consider this to be a two-dimensional problem, *i.e.*, we assume that everything is constant in the direction along the ice edge. The thickness of the oil is related to the oil volume, V, per meter of ice edge (linear volume, units m^2) and the oil slick length, X, by

$$V = hX. \tag{1}$$

Note also that all "forces" in this picture are given per meter of ice edge, and have units N/m. In order to calculate a physical force, one must return to three dimensions by multiplying with the length of the ice edge.

The oil slick is subject to several forces as shown in Fig. 1. These are the gravitational force, F_G, the buoyancy force, F_B, exerted by the water, the differential pressure force, F_P, the skin friction, F_S, and the form drag, F_F, generated by the water current. The buoyancy force on the oil, F_B, is given by:

$$F_B = \rho_w g(h - \delta)X, \tag{2}$$

where ρ_w is the density of water, and δ is the free-board of the oil relative to the water surface (see Fig. 1). The gravitational force, F_G, on the oil is:

$$F_G = -\rho g h X, \tag{3}$$

where ρ is the density of the oil, and the negative sign indicates the downwards direction of the force. When hydrostatic equilibrium is reached, all the forces are in balance. In the vertical direction, the buoyancy force exerted by the water on the oil slick compensates the force of gravity. Hence we have $F_B + F_G = 0$, and we can solve to find the free-board, δ, of the oil relative to the water surface:

$$\delta = h(\rho_w - \rho)/\rho_w. \tag{4}$$

The differential pressure force (pressure integrated over depth) between the oil and the water side is given by

$$\begin{aligned} F_p &= \int_0^h g\rho z\,\mathrm{d}z - \int_0^{h-\delta} g\rho_w z\,\mathrm{d}z \\ &= \frac{1}{2}g\rho h^2 - \frac{1}{2}g\rho_w(h-\delta)^2 \\ &= \frac{1}{2}g'\rho h^2 \end{aligned} \tag{5}$$

where $g' = g(\rho_w - \rho)/\rho_w$ is the reduced gravity.

The friction force is assumed to contain two terms, the skin friction, F_S, and the form drag, F_F (see Fig. 1). The skin friction generated by the current on the oil-water interface is given by:

$$F_S = -\frac{1}{2}\rho_w X C_S U^2 \tag{6}$$

and the form drag is:

$$F_F = -\frac{1}{2}\rho_w h C_F U^2 \tag{7}$$

where X is the length of the slick, U is the current velocity, C_S is the skin friction coefficient and C_F is the form drag coefficient. These coefficients are unknown and will be determined by fitting to experimental data (see Section 3). The negative sign indicates the direction of the friction forces being towards the ice.

At equilibrium, the sum of all forces is zero, so in the horizontal direction we have

$$F_S + F_F + F_P = 0. \tag{8}$$

For application in oil spill modelling, we need an expression that can be solved to find the slick length, X, or equivalently the thickness, h. By inserting the expressions for the three different forces in Eq. (8), we obtain a cubic equation for the slick thickness, h,

$$g'\rho h^3 - \rho_w U^2 C_F h^2 - \rho_w U^2 V C_S = 0. \tag{9}$$

When all the parameters are known, this equation can be solved for h by analytical or numerical means. An explicit expression for h is given in Appendix A.

By introducing the combined drag coefficient, $C_D = C_S + C_F h/X$, we can rewrite Eq. (9) into

$$g'\rho h^3 = \rho_w U^2 h X C_D. \tag{10}$$

Next, we introduce a length scale based on the linear volume, $L = \sqrt{V}$, and seek to obtain an equation for the dimensionless slick length X/L, by substituting the thickness $h = V/X = L^2/X$. We also introduce the Froude number, Fr, which is a dimensionless number that gives the relationship between the forces due to flow inertia and forces due to gravity, given by

$$\mathrm{Fr} = \frac{U}{\sqrt{g'L}}. \tag{11}$$

With these substitutions, we finally obtain

$$X/L = (\rho/\rho_w)^{1/3} C_D^{-1/3} \mathrm{Fr}^{-2/3}. \tag{12}$$

3. Experimental results compared to theory

Experiments were carried out in a linear flume with recirculating current. A floating barrier representing ice was placed in the flume, and oil was introduced at the surface in front of the barrier. A schematic presentation of the experimental setup is shown in Fig. 2. Four different oils were used, one marine gas oil (MGO), and three crude oils from the Norwegian Continental Shelf. The crudes were artificially weathered through evaporation under the assumption that they would spend some time at sea after release before encountering ice. The Wisting and Troll B crude oils were evaporated to 250 °C, and the Grane crude oil was prepared in two different batches, evaporated to 200 °C and 270 °C. Evaporation to 200 °C corresponds to approximately 12–24 hours at sea, and 250 °C corresponds to about 2–5 days, depending on weather

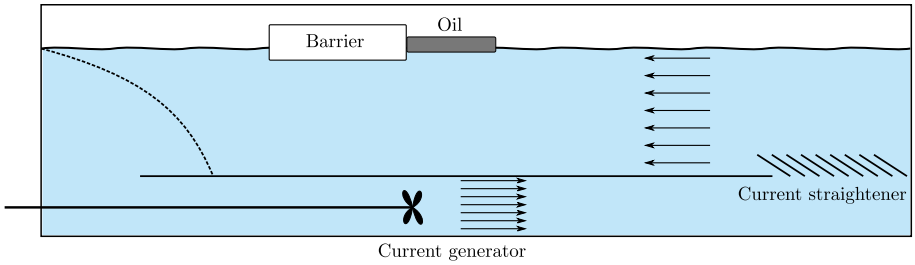

Fig. 2. Schematic presentation of the linear flume used in the experiments. The current is created by means of a propeller in a return channel below the main section of the flume. The length of the flume is 14 m, the water depth in the top section is approximately 1 m and the width of flume is 0.5 m.

Table 1
Densities and pour points of the different oils used in the experimental work. †Note that the pour point of Grane 270+ was not measured during the experiments. The table shows a previously measured value for Grane 250+, and the true value for Grane 270+ is probably higher.

Oil	Density [kg/m^3]	Pour point [°C]
MGO	852	< -36
Wisting 250+	883	< -36
Troll B 250+	922	-9
Grane 200+	950	-18
Grane 270+	967	$> -6^{\dagger}$

conditions (Daling et al., 1990). The densities and pour points of the oils are given in Table 1.

The flume was filled with filtered seawater (salinity 35 ppt). The entire flume is located in a temperature controlled room, and the temperature in the water was measured prior to each experiment. The temperature was between -0.8 °C and 0.5 °C in all cases in order to simulate water temperature conditions in ice-filled waters.

A weak current was applied, and the oil was poured onto the surface and allowed to collect in front of the barrier. After the oil had stabilised, typically after a few minutes, the extent, X, of the slick was measured. The current was then increased, and after the oil had stabilised, a new measurement was taken. In this manner, the measurements of slick length were repeated for different current speeds, U, different linear volumes of oil, V, and for oils with different densities, ρ. When the slick length is known, the slick thickness follows from Eq. (1), with the assumption of uniform thickness. Visual observations during the experiments indicated that the assumption of a constant thickness was reasonable in most cases (though see discussion in Section 5.1). The experimental design, and the results of the slick length measurements, are shown in Table 2.

3.1. Estimating the friction coefficients

Based on the results given in Table 2, the friction coefficients C_F and C_S were determined by fitting the theoretical dimensionless slick length (see Eq. (12)) to the data. We wrote a function taking the Froude number, Fr, as an argument, and returning the logarithm of the dimensionless length X/L, with C_F and C_S as adjustable parameters. The function curve_fit from the SciPy library (Virtanen et al., 2019) was then used to do a least squares fit to the experimentally measured values of $\log(X/L)$ as a function of Fr and determine the optimal parameter values.

Strictly speaking, there is one theoretical curve for each oil density. However, due to the relatively small variation in density between the oils considered, we chose to assume an average density of 914.8 kg/m^3, and fit a single curve to all the datapoints, obtaining the values $C_F = 0.151$, and $C_S = 0.00351$. The resulting curve is shown as a dashed line, together with the data in Fig. 3. The figure also shows the predicted dimensionless lengths for the densities 852 kg/m^3 and 967 kg/m^3, as the two dotted lines. We see that the variation due to density is far smaller than the variation seen between the different oils (and also within single oils), indicating that the majority of the variation in the data is due to other factors than density.

4. Implementation of thickness calculation

This section describes an implementation of surface oil thickness calculation in a particle-based oil spill model. We first describe an approach for oil in open water, and then how this could be modified in the

Table 2
Experimental design and results. For each oil, the slick length, X, in centimeters, is given for each combination of oil volume and current speed.

Oil linear volume [L/m]	Current [m/s]	MGO	Wisting 250+	Troll B 250+	Grane 200+	Grane 270+
5	0.05	95	150	170	100	–
5	0.10	95	100	100	70	85
5	0.15	85	90	75	55	70
5	0.20	70	60	55	25	65
5	0.25	55	45	35	20	30
10	0.05	250	220	280	170	150
10	0.10	160	150	140	120	125
10	0.15	130	120	110	40	70
10	0.20	100	80	60	35	50
10	0.25	80	60	45	30	–
20	0.05	355	350	340	295	315
20	0.10	255	220	210	185	190
20	0.15	190	170	140	80	80
20	0.20	150	110	80	45	65
20	0.25	120	90	60	–	–

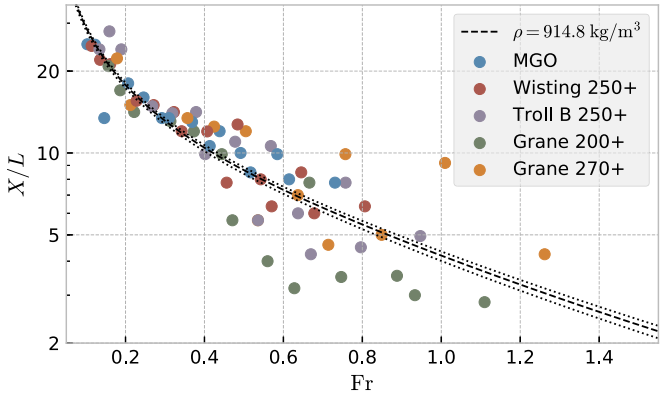

Fig. 3. Experimental results, showing dimensionless slick length, X/L, as a function of Froude number, Fr. The dashed line shows the best fit to the data (see Eq. (12)), assuming an average density of 914.8 kg/m^3, yielding the values $C_F = 0.151$ and $C_S = 0.00351$ for the two friction coefficients. The two dotted lines show the theoretical curves for densities 852 kg/m^3 and 967 kg/m^3 (assuming the same friction coefficients).

presence of ice, to make use of the results from Sections 2 and 3.

4.1. Lagrangian modelling

Numerical oil spill models usually employ a Lagrangian formulation, where the oil is represented by numerical particles,[1] also called Lagrangian elements (see, *e.g.*, Reed et al. (2000); French-McCay (2009)), which may represent oil spreading in the water column and as surface slicks. Here, we consider only particles on the ocean surface. Each particle represents a given mass of oil, and has properties such as a chemical composition and water content, which are regularly updated to account for weathering. From these properties, derived quantities such as viscosity may be obtained (Daling et al., 1990; Daling et al., 1997; Daling and Strøm, 1999). Furthermore, each numerical particle has a radius, representing its domain of influence as a disc on the ocean surface. The purpose of using finite size particles (as opposed to point particles) is to smoothe the aggregate quantities calculated from a collection of particles, such as slick thickness (see, *e.g.*, Silverman (1986); Lynch et al. (2014, Chapter 8)). The size of a particle will tend to grow with time, initially due to gravitational spreading and later due to horizontal turbulence.

4.2. Environmental input data

Environmental data are necessary to describe the forcing used to move particles in oil spill modelling. This includes wind, current, ice coverage and ice velocity, and sometimes additional parameters such as temperature, salinity, eddy diffusivity, *etc*. A coupled ice-ocean model with atmospheric forcing as input can provide this information, and the output is often available as gridded quantities in a netCDF format. For the example results presented in Section 4.4, we used data produced by the coupled ice-ocean model SINMOD (Slagstad and McClimans, 2005), with atmospheric forcing from ERA Interim (Dee et al., 2011). However, our approach for calculating oil thickness is general, and can be used with any source of environmental data as long as the required variables are available.

4.3. Oil thickness in open water

In a particle-based oil spill model, one may choose to assume that particles do not interact with each other. This greatly simplifies computation, but does carry some drawbacks. For example, when surface oil spreads under gravity, each particle would consider only its own thickness, while it would be more accurate to calculate spreading using an aggregated thickness calculated from all overlapping particles. In open water, this distinction is usually not very important, as the oil will quickly become so thin or weathered that gravity spreading is no longer the dominant diffusion mechanism.

The thickness of a surface oil particle is given by

$$h = \frac{V}{4\pi r^2}, \tag{13}$$

where h is the thickness of the particle, V is the volume of oil (emulsion) represented by that particle, and r is its radius.

When calculating the aggregate oil thickness from several particles, the particles are usually projected onto a grid. Each particle that overlaps with a cell contributes a fraction of its mass to that cell, and the volume of emulsion in the cell, V_e, is simply the sum of these contributions. Finally, the oil thickness in the surface grid cell, H, is deduced:

$$H = \frac{V_e}{(\Delta x)^2} \tag{14}$$

where $(\Delta x)^2$ is the area of the cell.

We note that the thickness, h, of each individual particle, is calculated independently of all other particles, while the aggregate thickness, H, on the grid also depends implicitly on the density of particles. Hence, the aggregate thickness is affected by processes such as differential advection by currents, and horizontal diffusion (usually modelled as a random walk). These processes can cause the oil to spread out to cover large areas over time.

4.4. Oil thickness at the ice edge

In the presence of an ice edge, the oil can be forced against the edge by the current or wind and increase in thickness. However, the thickness calculation described in Section 4.3 does not take gravity spreading into account in the bulk oil, only independently in each particle. Hence, this approach can give unrealistic predictions of slick thickness when a large number of particles are collected in the same area of the ice edge. In the theoretical model described in Section 2, the thickness will only increase until the compressing drag forces are balanced by the internal pressure (due to gravity) in the oil.

For calculating the thickness of oil at the ice edge, we propose an implementation consisting of these steps:

1. Identify the location of the ice edge.
2. Find the on-ice component of the relative current.
3. Identify those oil particles that are at the ice edge.
4. Calculate the linear volume of oil at the edge.
5. Calculate the oil thickness from Eq. (9).

To illustrate the different steps of the implementation, we have simulated an oil spill scenario where oil is spilled in open water, and drifts into the ice edge. We have used the OSCAR oil spill model (Reed et al., 2000; Nordam et al., 2018; Nordam et al., 2019), and simulated

Table 3
Description of the scenario used to illustrate the different implementation steps of the oil thickness calculation.

Oil type	Troll
Oil density	893 kg/m^3
Release location	76.999°N, 32.752°E
Release depth	0 m
Release rate	19,200 m^3/day
Release duration	4 days
Simulation start time	2009-03-08, 00:00:00
Simulation duration	7 days

[1] Whenever we use the term "particle", we mean numerical particle.

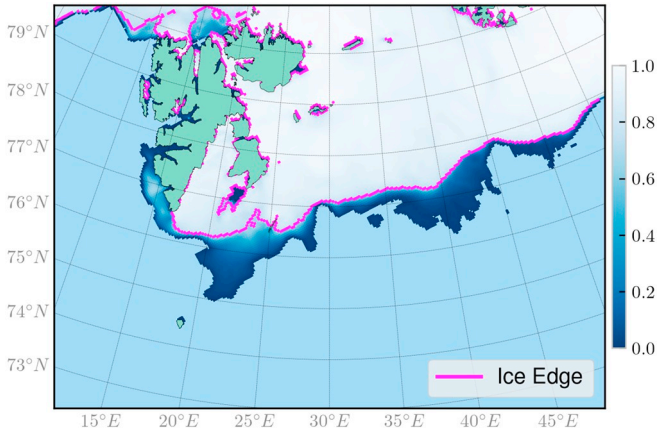

Fig. 4. Illustration of an ice edge, as defined in Section 4.4, using modelled ice coverage fraction for the Barents Sea, on March 14, 2009.

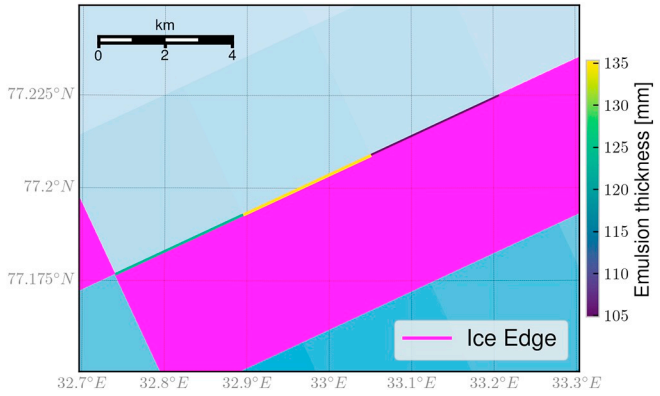

Fig. 6. Calculated thickness of surface oil at the ice edge. Within one cell of the ice grid, the oil is assumed to consist of a narrow band of constant width and thickness, and the width is shown to scale.

the (fictional) scenario described in Table 3. The release rate is set high to ensure sufficient oil encountering ice, but lies within the range of what is recommended for use in environmental risk analysis on the Norwegian continental shelf (Nilsen et al., 2014). The environmental input data was produced by the SINMOD coupled ice-ocean model (Slagstad and McClimans, 2005), and has 4 km horizontal resolution.

In our model, we propose to define the ice edge to consist of those grid cells where the ice coverage is lower than 70% and at minimum one nearest-neighbor cell has an ice coverage greater than or equal to 70%. The choice of the threshold to define the ice edge is motivated by the rule-of-thumb stating that oil cannot move independently of the ice when the coverage is above 80% (El-Tahan et al., 1988; Venkatesh et al., 1990). With oil-in-ice transport implemented according to the rule-of-thumb, as described by Nordam et al. (2019), we find that the oil will in practice stop at concentrations a little below 80%, hence we chose to use 70% to define the ice edge. This approach to identifying the ice edge is shown in Fig. 4 for the last day of the scenario described in Table 3.

To solve Eq. (9) for the oil thickness, h, we need to find the current pushing the oil against the ice edge. We calculate the relative current velocity vector,

$$\mathbf{U}_{rel} = \mathbf{U} - \mathbf{U}_{ice} \tag{15}$$

where $\mathbf{U}$ is the surface current velocity and $\mathbf{U}_{ice}$ the ice velocity, as provided by the coupled ice-ocean model. We then find the on-ice normal component of the relative current, *i.e.*, the component of the relative current that is orthogonal to the ice edge. The details of this calculation will depend on the grid projection used by the ice-ocean model, and the basis on which the current and ice velocity vectors are defined.

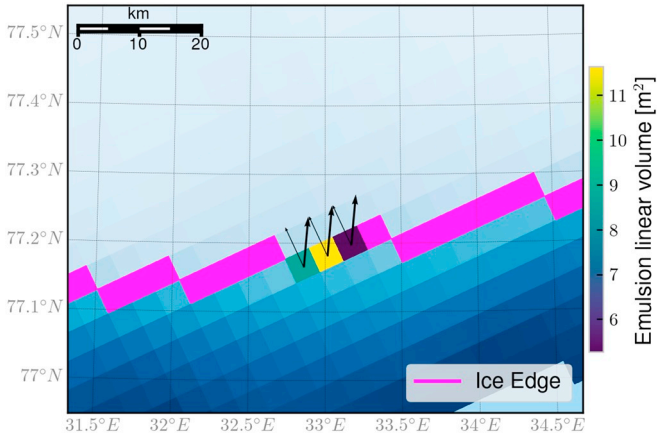

Fig. 5. Example of linear emulsion volume in ice edge cells. Also shown is the relative current (Eq. (15), shown as thick arrows), and the normal (on-ice) component of the relative current (thin arrows).

Next, we identify those particles that are in the ice-edge cells, using the center of the disc shaped particles to determine their position. To find the volume of emulsion in an ice-edge cell, we simply add the volumes represented by all the particles whose centers are inside that cell. We then find the linear volume by dividing with the length of the cell edge, Δx. To solve for the thickness, we also need the density of the emulsion. This is calculated by volume-weighted average over all the particles contributing to each cell. Fig. 5, shows the calculated linear volume of oil at the ice edge as well as the normal component of the relative current at the end of the scenario described in Table 3.

With all the above information, the final step is to solve Eq. (9) for the slick thickness, h, which also gives the extent of the slick, X, by Eq. (1), as the linear volume is known. Note that we now no longer assume that the oil is evenly distributed throughout the cell, but rather that the oil is located in a narrow band, of width X and thickness h, along the edge of each ice-edge cell. The thickness of surface oil obtained at the end of the example scenario is illustrated in Fig. 6.

5. Discussion

We have described an approach for calculating the thickness of surface oil being forced against an ice edge (or other floating barrier) by currents. The need for such an approach comes from the fact that Lagrangian particle models with non-interacting particles are unable to calculate a physics-based surface oil thickness when particles encounter a barrier. In this case, the thickness should be calculated by considering the balance between the forces that lead to a collection of particles, and the retarding force of gravity spreading. Neglecting to take this force balance into account can lead to over- or underprediction of surface slick thickness, depending on the scenario and the resolution of the surface grid.

We note that our approach for describing oil being pushed against an ice edge is fundamentally different from a description of oil being pushed against the shoreline, since the current can flow under the ice, but cannot flow into the shore. In that sense, oil being pushed against an ice edge shares similarity with oil being collected in a boom.

5.1. Comparison to experimental results

Our theory is compared to experimental results from a linear flume with recirculating current. A reasonable match is found between experimental results and theory, as shown in Fig. 3, though there is some scatter in the experimental data, with larger variability between each oil than would be predicted through differences in density alone. The

theory was developed with the assumptions of a Newtonian fluid, steady state constant thickness, and constant conditions in the direction parallel to the ice edge. We believe the two most likely reasons for deviations between the model and results are adhesion between the oil and the side of the flume, and non-Newtonian behaviour of the oil.

Oil adhering to the sides of the flume is expected to give rise to longer slick lengths than predicted by the theory, as the adhesion provides an additional force not accounted for in Eq. (8). The adhesive force will behave like a friction force, acting to preventing any change of slick length, both compression and elongation. However, as the experiments were all started from a long slick, which was gradually compressed as the current was increased in steps, the net result of the adhesion is a larger slick length.

The effect of non-Newtonian behaviour is also to resist deformation of the slick. Assuming that a non-Newtonian oil acts like a Bingham-fluid (see, *e.g.*, Brönner et al. (2018)), it will not flow unless the stress exceeds the limit given by the yield stress. In the experiments described here, the effect of any non-zero yield stress will be more noticeable for the smaller linear volumes used in the experiments. The reason is that the friction forces from the moving water will increase both with the slick length and the slick thickness, while the force required to overcome the yield stress is only dependent on the slick thickness.

Furthermore, a non-zero yield stress will affect the friction terms of the force balance, by allowing the leading edge of the oil to take and keep different deformed shapes. Hence, the net effect of non-Newtonian behaviour is somewhat unpredictable. Experiments were also carried out with highly non-Newtonian emulsions at 50% water content and above, but the results are not reported here, for the reasons just described. See Singsaas et al. (2020) for details.

In all of the experiments, the temperature was above the pour point of the oil (see Table 1), but not always by a large margin. Non-Newtonian behaviour, as may be caused by wax precipitation, can occur for temperatures above the pour point. We expect any deviation due to non-Newtonian behaviour to be most significant for the oils with the highest pour points. As discussed above, we also expect those experiments with the smallest linear volumes to be most sensitive to non-zero yield stresses. If we exclude the two oils with the highest pour points, Troll B 250+ and Grane 270+, and we also exclude the experiments with a linear volume of 5 L/m, we obtain the results shown in Fig. 7. The dashed line is a best fit to only the datapoints shown, giving somewhat different values for the drag coefficients. The reduced scatter in the experimental data supports our discussion of the sources of error.

5.2. Applicability of the model to real conditions

In the derivation of the equation for oil thickness against an ice edge, we made several simplifications. The most obvious is perhaps that we approximate the “ice edge” as a straight barrier. In reality, the transition from open water to full ice cover may take a large range of different forms, with details at a scale that is difficult or impossible to capture in an ice-ocean model. The rationale behind the assumption of a straight ice edge, aside from the simplicity, is that in a situation where the oil is pressed against the main body of the ice, the MIZ will probably also be compressed, leading to a relatively sharp transition from open water to full ice cover. However, the effect of the oil already being in partial ice cover, prior to the compression of the MIZ, is not taken into account. Another assumption is that the oil slick has a constant thickness. It is not known how well this will hold up under field conditions, and particularly for large slicks.

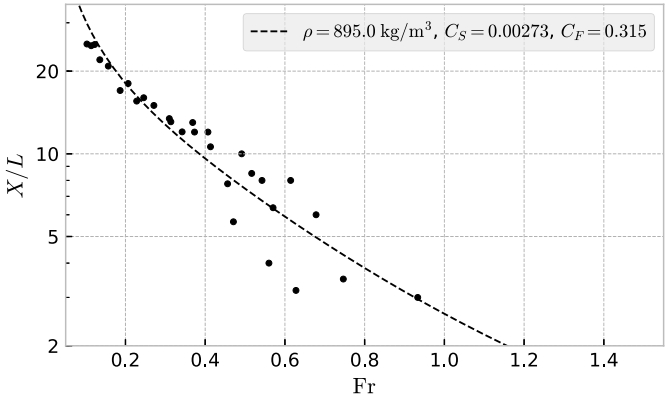

Fig. 7. The dashed curve was fit to the reduced dataset with least squares, assuming a constant density of 895 kg/m^3, which is the average of the three oils used. From this, we obtained the values of the two friction coefficients, $C_F = 0.315$, and $C_S = 0.00273$.

In addition to the previously discussed non-Newtonian behaviour, which is certainly relevant for many crude oil emulsions, other factors not taken into account include the direct effect of wind and waves on the oil. Wind might be relatively straightforward to take indirectly into account, by considering the commonly used ~3% windage factor for the transport of surface oil (see, *e.g.*, Simecek-Beatty (2011)) as a contribution to the surface current. No experimental work was done with wind in this study, but this would be an interesting direction to explore in the future.

The effect of waves on the oil is far more difficult to take into account. In addition to the Stokes drift, which may give an additional contribution to the current, there is also the wave-damping effect of the oil. Due to the conservation of momentum, any damping of waves gives rise to a force that will act to further compress the oil. This was not explored in detail in the experimental work, but some preliminary tests indicated significant sensitivity to oil volume and viscosity, and the amplitude and wavelength of the waves. Any reflection of waves from the barrier also seemed to play an important role, and this will in practice be completely dependent on the detailed conditions in the transition from open water to full ice cover, on a scale much smaller than the 1 to 4 km resolution currently available in regional coupled ice-ocean models.

The application of the model should take the assumptions made in the derivation into account, and only apply these calculations when the oil is predicted to be in a Newtonian state. For a spilled oil, this will vary by oil type and degree of weathering, which means that a sufficient description of oil characteristics and weathering fate to infer this information is required. Finally, given that oil that has spent some time at sea is likely to exist in the form of a non-Newtonian emulsion, it is clearly of some interest to establish theory and supporting experiments to predict thickness in these cases as well.

6. Conclusion

Prediction of surface oil thickness is a fundamental challenge in oil spill modelling. Here, we have focused on the calculation of oil thickness for the situation where oil is collected by ocean currents against an ice barrier. Based on the force balance, and under the assumption of Newtonian fluid, a model of oil thickness in the presence of an ice edge is established. Using two fitted friction coefficients, a reasonable match to the experimental data is achieved. We also propose an implementation of the oil thickness calculation at the ice edge in particle based oil spill models, taking commonly available data through coupled ice-ocean models as input. This approach should increase the physical realism of oil spill models near an ice edge and may also be applied to other situations in which oil encounters a floating barrier. Further experiments with applied wind and wave forcing, as well as non-Newtonian emulsions, should be explored in order to investigate the impacts of these forces on oil film thickness near a barrier.

CRediT authorship contribution statement

Tor Nordam: Conceptualization, Methodology, Software, Formal analysis, Writing - original draft, Writing - review & editing, Visualization, Project administration. **Emma Litzler**: Software,

Writing - original draft, Writing - review & editing, Visualization. **Jørgen Skancke**: Formal analysis, Writing - original draft, Writing - review & editing. **Ivar Singsaas**: Methodology, Investigation, Data curation, Project administration. **Frode Leirvik**: Methodology, Investigation, Data curation. **Øistein Johansen**: Conceptualization, Methodology, Formal analysis, Supervision.

Declaration of competing interest

The authors declare that they have no known competing financial interests or personal relationships that could have appeared to influence the work reported in this paper.

Acknowledgements

The work presented was carried out under the FateIce project (255385/E30), supported by the PETROMAKS2 programme of the Norwegian Research Council, and by AkerBP, ConocoPhillips, Equinor, Lundin Norway, Neptune Energy, OMV, and Vår Energi.

Appendix A. Solution to cubic equation for slick thickness

The cubic equation for oil slick thickness, Eq. (9), can be solved numerically or analytically. We chose to solve it analytically, using the SymPy symbolic mathematics library for Python (Meurer et al., 2017). This equation has three roots, but two of them are complex, and thus do not correspond to physical solutions for the slick thickness, h. The third solution gives a real value of h, given by

$$h = -\frac{1}{3}\sqrt[3]{\frac{1}{2}\sqrt{\left(-\frac{27d}{a}-\frac{2b^3}{a^3}\right)^2-\frac{4b^6}{a^6}}-\frac{27d}{2a}-\frac{b^3}{a^3}}+\frac{b}{3a}-\frac{b^2}{3a^2\sqrt[3]{\frac{1}{2}\sqrt{\left(-\frac{27d}{a}-\frac{2b^3}{a^3}\right)^2-\frac{4b^6}{a^6}}-\frac{27d}{2a}-\frac{b^3}{a^3}}}, \tag{A.1a}$$

where we have used the following substitutions:

$$a = g'\rho, \tag{A.1b}$$

$$b = \rho_w U^2 C_F, \tag{A.1c}$$

$$d = \rho_w U^2 V C_S. \tag{A.1d}$$

References

Afenyo, M., Khan, F., Veitch, B., Yang, M., 2016a. Modeling oil weathering and transport in sea ice. Mar. Pollut. Bull. 107 (1), 206–215.

Afenyo, M., Veitch, B., Khan, F., 2016b. A state-of-the-art review of fate and transport of oil spills in open and ice-covered water. Ocean Eng. 119, 233–248.

Arneborg, L., Höglund, A., Axell, L., Lensu, M., Liungman, O., Mattsson, J., 2017. Oil drift modeling in pack ice–sensitivity to oil-in-ice parameters. Ocean Eng. 144, 340–350.

Bagi, A., Pampanin, D.M., Brakstad, O.G., Kommedal, R., 2013. Estimation of hydrocarbon biodegradation rates in marine environments: a critical review of the Q10 approach. Mar. Environ. Res. 89, 83–90.

Brandvik, P.J., Faksness, L.-G., 2009. Weathering processes in Arctic oil spills: meso-scale experiments with different ice conditions. Cold Reg. Sci. Technol. 55, 160–166.

Brönner, U., Johansen, Ø., Leirvik, F., Nordam, T., Sørheim, K.R., 2018. Spreading of waxy oils on calm water. Mar. Pollut. Bull. 129 (1), 135–141.

Daling, P.S., Strøm, T., 1999. Weathering of oils at sea: model/field data comparisons. Spill Sci. Technol. Bull. 5 (1), 63–74.

Daling, P.S., Brandvik, P.J., Mackay, D., Johansen, Ø., 1990. Characterization of crude oils for environmental purposes. Oil Chem. Pollut. 7 (3), 199–224.

Daling, P.S., Aamo, O.M., Lewis, A., Strøm-Kristiansen, T., 1997. SINTEF/IKU oil-weathering model: predicting oils' properties at sea. In: Proceedings of the 1997 International Oil Spill Conference. 1997. pp. 297–307.

Dee, D., Uppala, S., Simmons, A., Berrisford, P., Poli, P., Kobayashi, S., Andrae, U., Balmaseda, M., Balsamo, G., Bauer, P., et al., 2011. The ERA-interim reanalysis: configuration and performance of the data assimilation system. Q. J. R. Meteorol. Soc. 137 (656), 553–597.

El-Tahan, H., Comfort, G., Abdelnour, R., 1988. Development of a Methodology for Computing Oil Spill Motion in Ice-Infested Waters. Rep. Submitted by Fleet Technology Limited, Kanata, Ont., to Atmospheric Environment Service, Downsview, Ont.

French-McCay, D.P., 2009. Oil spill impact modeling: development and validation. Environ. Toxicol. Chem. 23 (10), 2441–2456.

French-McCay, D., Gearon, M.S., Kim, Y.H., Jayko, K., Isaji, T., 2014. Modelling oil transport and fate in the Beaufort Sea. In: Proceedings of the 37th AMOP Technical Seminar, Ottawa, ON, Canada. Environment Canada, pp. 40–64.

French-McCay, D.P., Tajalli-Bakhsh, T., Jayko, K., Spaulding, M.L., Li, Z., 2018. Validation of oil spill transport and fate modeling in Arctic ice. Arctic Sci. 4 (1), 71–97. URL. setac.onlinelibrary.wiley.com/doi/abs/10.1897/03-382.

Lofthus, S., Netzer, R., Lewin, A.S., Heggeset, T.M., Haugen, T., Brakstad, O.G., 2018. Biodegradation of n-alkanes on oil–seawater interfaces at different temperatures and microbial communities associated with the degradation. Biodegradation 29, 141–157.

Lynch, D.R., Greenberg, D.A., Bilgili, A., McGillicuddy Jr., D.J., Manning, J.P., Aretxabaleta, A.L., 2014. Particles in the Coastal Ocean: Theory and Applications. Cambridge University Press.

Meurer, A., Smith, C.P., Paprocki, M., Čertík, O., Kirpichev, S.B., Rocklin, M., Kumar, A., Ivanov, S., Moore, J.K., Singh, S., Rathnayake, T., Vig, S., Granger, B.E., Muller, R.P., Bonazzi, F., Gupta, H., Vats, S., Johansson, F., Pedregosa, F., Curry, M.J., Terrel, A.R., Roučka, V., Saboo, A., Fernando, I., Kulal, S., Cimrman, R., Scopatz, A., Jan. 2017. SymPy: symbolic computing in python. PeerJ Comput. Sci. 3, e103.

Nilsen, T., Jacobsen, N.E.B., Myhrvold, A., Nilsen, E.F., Roald, T., 2014. Guidance on Calculating Blowout Rates for Use with Environmental Risk Analyses. Tech. rep. Norwegian Oil and Gas.

Nordam, T., Dunnebier, D.A.E., Beegle-Krause, C.J., Reed, M., Slagstad, D., 2017. Impact of climate change and seasonal trends on the fate of Arctic oil spills. AMBIO 46, 442–452.

Nordam, T., Litzler, E., Rønningen, P., Aune, J., Hagelien, T.F., Loktu, A., Beegle-Krause, C.J., Brönner, U., 2018. Oil spill contingency and response modelling in ice-covered waters. In: Proceedings of the 41st AMOP Technical Seminar. Environment Canada, Victoria, BC, Canada.

Nordam, T., Beegle-Krause, C.J., Skancke, J., Nepstad, R., Reed, M., 2019. Improving oil spill trajectory modelling in the Arctic. Mar. Pollut. Bull. 140, 65–74.

Nordam, T., Lofthus, S., Brakstad, O.G., 2020. Modelling biodegradation of crude oil components at low temperatures. Chemosphere 254, 126836.

Reed, M., Daling, P.S., Brakstad, O.G., Singsaas, I., Faksness, L.-G., Hetland, B., Ekrol, N., 2000. OSCAR 2000: a multi-component 3-dimensional oil spill contingency and response model. In: Proceedings of the 23rd AMOP Technical Seminar. 2000. Environment Canada, Vancouver, Canada, pp. 663–680.

Silverman, B.W., 1986. Density Estimation for Statistics and Data Analysis. Chapman & Hall.

Simecek-Beatty, D., 2011. Oil spill trajectory forecasting uncertainty and emergency response. In: Fingas, M. (Ed.), Oil Spill Science and Technology. Gulf Professional Publishing, Boston, pp. 275–299.

Singsaas, I., Leirvik, F., Daling, P.S., Guénette, C., Sørheim, K.R., 2020. Fate and Behaviour of Weathered Oil Drifting into Sea Ice, Using a Novel Wave and Current Flume. (Submitted to Marine Pollution Bulletin).

Slagstad, D., McClimans, T.A., 2005. Modeling the ecosystem dynamics of the Barents Sea including the marginal ice zone: I. Physical and chemical oceanography. J. Mar. Syst. 58, 1–2, 1–18.

Venkatesh, S., El-Tahan, H., Comfort, G., Abdelnour, R., 1990. Modelling the behaviour of oil spills in ice-infested waters. Atmosphere-Ocean 28, 303–329.

Virtanen, P., Gommers, R., Oliphant, T.E., Haberland, M., Reddy, T., Cournapeau, D., Burovski, E., Peterson, P., Weckesser, W., Bright, J., van der Walt, S.J., Brett, M., Wilson, J., Jarrod Millman, K., Mayorov, N., Nelson, A.R.J., Jones, E., Kern, R., Larson, E., Carey, C., Polat, I., Feng, Y., Moore, E.W., Vand erPlas, J., Laxalde, D., Perktold, J., Cimrman, R., Henriksen, I., Quintero, E.A., Harris, C.R., Archibald, A.M., Ribeiro, A.H., Pedregosa, F., van Mulbregt, P., et al., Jul 2019. SciPy 1.0–Fundamental Algorithms for Scientific Computing in Python. arXiv:1907.10121.